INTERNATIONAL JOURNAL OF SUSTAINABLE CONSTRUCTION ENGINEERING AND TECHNOLOGY
VOL. 14 NO. 4 (2023) 412-425

IJSCET

http://publisher.uthm.edu.my/ojs/index.php/ijscet

ISSN : 2180-3242 e-ISSN : 2600-7959

International Journal of Sustainable Construction Engineering and Technology

Analysis of Indonesia's Railway Track Structure Behavior Under Double-Stack Freight Train Loading

Hanafi Isnanta Prabawa[1*]

[1]Research Center for Transportation Technology,
National Research and Innovation Agency of Indonesia, Jakarta, INDONESIA

*Corresponding Author

DOI: https://doi.org/10.30880/ijscet.2023.14.04.030
Received 28 April 2023; Accepted18 December 2023; Available online 28 December 2023

Abstract: The growing number of freight transported using railway transport is massive. Indonesia targeted 995,500,000 tons of freight transported using the railway mode. Double-stack train is one solution to increase the freight tonnage of the train without adding the number of operations of the train. The 3D ANSYS model is made to see the structural behavior of railway tracks under the double-stack train load using 1067 mm and 1435 mm gauge from Indonesia's railway track regulation. It was also modeled with several speeds to observe its influence on the structure. It is known that in all output parameters of deformation, stress, and strain, the 1435 mm gauge acts better for the structure than the 1067 mm gauge. The subgrade service life also became longer in the 1435 mm gauge structure. Lower speed also gives a better impact on the structure of the track and possible to give longer service life for subgrade. Further research is needed to observe the railway track structural behavior in cyclic loading and the possibility of reinforcing the subgrade. The lab-scale test also needed to validate the analysis.

Keywords: Railway track, structure behavior, Double-Stack Train, ANSYS, service life

1. Introduction

The Railway is an essential transportation mode to transport passengers and freights worldwide. In 2006, the contribution of rail-based transportation mode in Indonesia is still lower than road-based transportation, with only 7.32% of passenger transportation and 0.63% of freight transportation (Muthohar et al., 2009). However, it is increasing in recent years. In 2022, 61.9 million tons of commodities are transported through railway lines, as well as 277 million passengers (Badan Pusat Statistik, 2023). In addition, the Indonesian Government projected that in 2030 there will be 929,500,000 people and 995,500,000 tons of freight transported using railway services (Kementerian Perhubungan, 2018). The increasing of passengers and freights transported means more cars to operate. To accommodate that, railway operators should add more cars to each train set or increase the number of trains. On the other hand, these strategies have many disadvantages for the train operation. Increasing the number of cars on every trainset will increase the length of a trainset, thus the train driver will be difficult to monitor the trainset until the last car and causing an issue for the safety factor. Furthermore, increasing the length of emplacement is also needed to accommodate passengers' boarding and alighting or loading and unloading freight, causing more expense to develop the station area. Increasing the number of trains will also affect railway traffic, especially on the lines with heavy traffic. It will be more difficult for the scheduler to make a timetable, causing the schedule's risk of not being as actual as the timetable.

Another solution to overcome the problem, especially in freight trains, is by operating double-stack cars for container freight trains. Double-stack trains are normally used for container freight trains, because of the ease to be stacked on the cars. Most double-stack cars use 40 ft or 53 ft container size, and they also can be stacked with several

*Corresponding author: hanafi.isnanta.prabawa@brin.go.id

configurations. As shown in Fig 1, the bottom position can be loaded by 2x20 ft containers or a single 40 ft container while the upper position can be loaded by 40 ft or higher cube size i.e. 45 ft, 48 ft, or 53 ft container to maximize the use of space in the cars. However, the central position of the upper container must be symmetrically connected to the central point of the bottom container (Mantovani et al., 2018). Double-stack trains are first operated in 1977 and until today widely used in The United States, Australia, India, and other countries (Alam & Watkins, 2007; Ng & Talley, 2020). This type of train gives many advantages; it can carry more containers than a conventional one without increasing the number of cars, locomotives, and crew, and it also gives a smooth cargo ride thus minimizing vibration for the commodities (Urban, 1987). In addition, operating double-stack trains provides many advantages for the environment. For example, the pollution caused by the operation of double-stack trains is lower than the operation of regular freight trains with an equal number of transported containers because double-stack trains offer fewer trainsets to operate than regular freight trains. Several studies regarding double-stack trains have been delivered. (Mantovani et al., 2018; Ng & Talley, 2020; Ruf et al., 2022) have modeled the load planning of double-stacked trains in a container terminal. While (Alam & Watkins, 2007) investigated the behavior of double stacked-train due to crosswind effects during the trip. However, there are still few articles investigating the effect of the operation of double-stacked trains on the railway track.

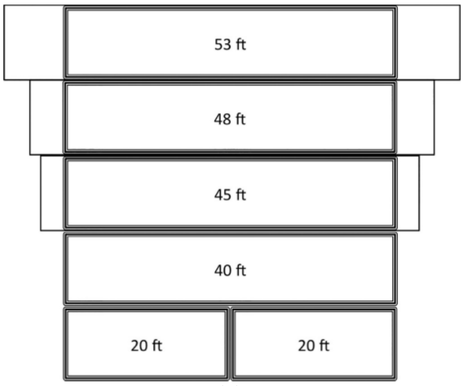

(a)

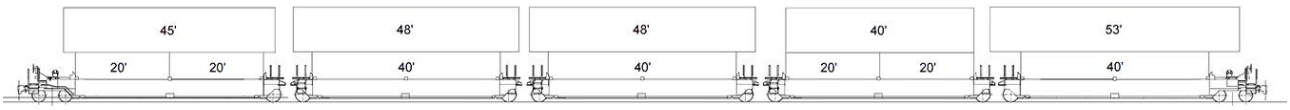

(b)

Fig. 1 - Container Stacking Configuration in Double-Stack Freight Train: (a) Arrangement of stacking (Mantovani et al., 2018); (b) Example of stacking for different configurations in a trainset (www.gbrx.com, 2022)

Railway tracks are distinguished into the ballasted track and ballastless track, presented in Fig 2. Ballasted track, well known as the conventional railway track, is a track structure consisting of rails and sleepers supported on the ballast. This type of track has appeared since the beginning of the invention of the railways. The ballasted track has many advantages due to the low initial construction cost and convenience of the construction process. However, it also has several drawbacks such as the dynamic stability is not as good as the ballastless track, and it also needs higher maintenance frequency (Esveld, 2001). Meanwhile, a ballastless track, or so-called slab track, is a track structure that replaces the ballast layer on ballasted track with a concrete or asphalt layer. The ballastless track is mainly used in high-speed railways and light railways. The advantages of this type of track are giving better dynamic stability and a smooth ride for the trains, and it also has less maintenance frequency. Meanwhile, the disadvantage of this track is the high initial construction cost (Michas, 2012).

Indonesia's railway tracks are mainly using ballasted tracks, especially on the railway line used for intercity passenger trains and freight trains. The design of Indonesia's railway track refers to the Minister of Transportation Regulation No. 60 of 2012 About the Technical Requirement of Railways (Kementerian Perhubungan, 2012). On the regulation, Indonesia uses 2 types of gauge, which are narrow gauge (1067 mm) and standard gauge (1435 mm). Each gauge has several rail track classes that are related to the tonnage passed, maximum speed, sleeper type, and ballast thickness as shown in Table 1 and Table 2.

As presented in Table 1 and Table 2, 18 tons of axle load is applied in all rail track classes for 1067 mm gauge, while 22.5 tons of axle load is applied in all rail track classes for 1435 mm gauge. This determination does not consider performance for each component layer, thus the fatigue point and service life of the railway tracks are not known.

(a) (b)

Fig. 2 - Different types of railway track structure: (a) Ballasted track; (b) Ballastless track

Table 1 - Classification of Indonesia Railway Track for 1067 mm gauge (Kementerian Perhubungan, 2012)

Rail Track Class	Passing Tonnage (Tons/Year)	Design Speed (Km/Hour)	Axle Load (Tons)	Rail Type	Sleeper Type / Distance Between Sleeper (mm)	Ballast Thickness (mm)
I	> $20x10^6$	120	18	R.60/R.54	Concrete / 600	300
II	$10x10^6$ – $20x10^6$	110	18	R.54/R.50	Concrete/Timber / 600	300
III	$5x10^6$ – $10x10^6$	100	18	R.54/R.50/R.42	Concrete/Timber/Steel / 600	300
IV	$2.5x10^6$ – $5x10^6$	90	18	R.54/R.50/R.42	Concrete/Timber/Steel / 600	250
V	< $2.5x10^6$	80	18	R.42	Timber/Steel / 600	250

Table 2 - Classification of Indonesia Railway Track for 1435 mm gauge (Kementerian Perhubungan, 2012)

Rail Track Class	Passing Tonnage (Tons/Year)	Design Speed (Km/Hour)	Axle Load (Tons)	Rail Type	Sleeper Type / Distance Between Sleeper (mm)	Ballast Thickness (mm)
I	> $20x10^6$	160	22.5	R.60	Concrete / 600	300
II	$10x10^6$ – $20x10^6$	140	22.5	R.54	Concrete / 600	300
III	$5x10^6$ – $10x10^6$	120	22.5	R.60/R.54	Concrete / 600	300
IV	< $5x10^6$	100	22.5	R.60/R.54	Concrete / 600	300

Several studies regarding the evaluation of railway tracks have been presented by (Liu, 2013; Rose et al., 2014; Rose & Souleyrette, 2016; Setiawan, 2021, 2022) using KENTRACK software found that the stress on the top of the subgrade will reduce with the adding asphalt layer between ballast and sub-ballast thus will extend the service life. KENTRACK output is the maximum compressive stress and designs life of the subgrade. However, this software has a drawback, the distribution of the stress and the vertical deformation is unknowable. (Kalliainen et al., 2016) studied the behavior of railway tracks using Plaxis 3D with several specifications of rail, rail pads, sleeper, ballast, sub-ballast, frost protection layer, and subgrade. While (M. Setiawan, 2022) evaluate the 1067 mm Indonesia's railway track performance 2D simulation using ABAQUS software with several combinations of speed and axle load.

There are several cars used to transport logistics in Indonesia. A flat car used for transport containers with several capacities i.e. 42 tons, 45 tons, and 54 tons. Open wagons are used for transporting bulk commodities such as coal with a capacity of 50 tons, while tank cars are used for transporting liquid commodities such as gasoline with a capacity of up to 40 tons. However, double-stack cars give a higher load capacity of up to 77 tons. Even though double-stack trains are never used before in Indonesia, but within all the advantages, it is possible that the double-stack train will be operated in Indonesia with the number of containers transported by train is more than 4 million tons and continuously growing (PT. Kereta Api Indonesia, 2022). With the big maximum load differentiation between cars used in Indonesia and double-stack cars, it is really important to understand the behavior of the railway track under the double-stack trains loading, thus will understand the readiness of the railway track to be used, in this case, based on Indonesia's regulation, and this will help the railway stakeholder in Indonesia decide the operation of double-stack trains and make sure about the safety of the track.

2. Research Method

In this case, to analyze the behavior of the railway track is simulated using 3D model ANSYS 2023 software. The model, material properties, and load used in the simulation will be explained.

2.1 Railway Track Dimension

1067 mm gauge model and 1435 mm gauge model are used to be evaluated in this simulation. All track types use the 1st rail track class on each classification and the dimension of every track layer is presented in Table 3 and Table 4 based on Indonesia's Railway Technical Requirements. Fig 3 and Fig 4 show the dimension of each model and also show the measurement point of vertical displacement, equivalent stress, and strain.

Table 3 - Dimension model of 1067 mm gauge railway track layer

Track Layers	Dimension (mm) LxWxH
Sleeper	2000 x 260 x 220
Ballast	4700 x 1000 x 300
Sub-Ballast	4700 x 1000 x 400
Subgrade	4700 x 1000 x 2800

Table 4 - Dimension model of 1435 mm gauge railway track layer

Track Layers	Dimension (mm) LxWxH
Sleeper	2740 x 330 x 220
Ballast	4700 x 1000 x 300
Sub-Ballast	4700 x 1000 x 400
Subgrade	4700 x 1000 x 2800

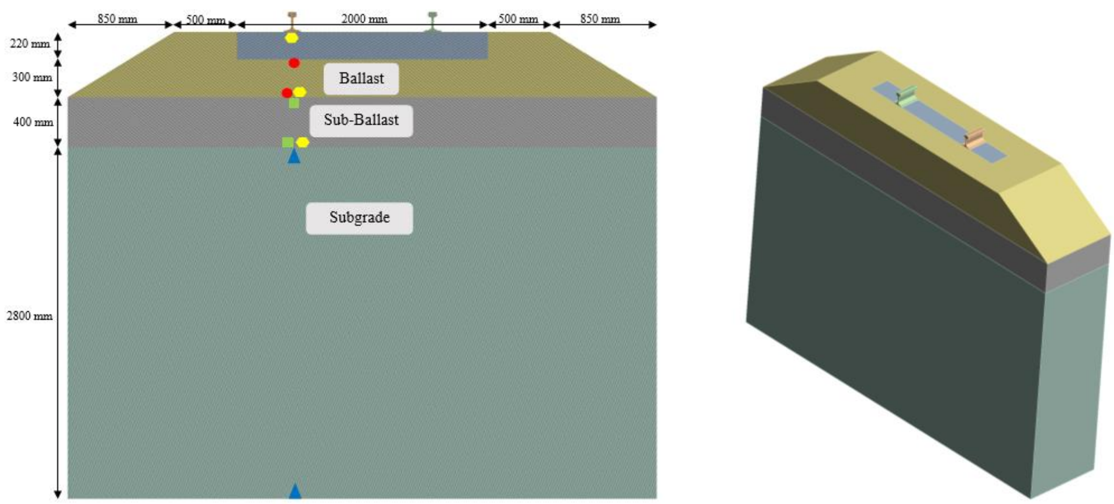

(a) (b)

- Strain-Stress at the top and bottom of ballast
- Strain-Stress at the top and bottom of sub-ballast
- Strain-Stress at the top and bottom of subgrade
- Deformation at the top of sleeper, at the bottom of ballast, and at the bottom of sub-ballast

Fig. 3 - Dimension Model of 1067 mm Gauge Railway Track: (a) Cross Section Model Dimension and Measuring Point; (b) 3D Model for Analysis

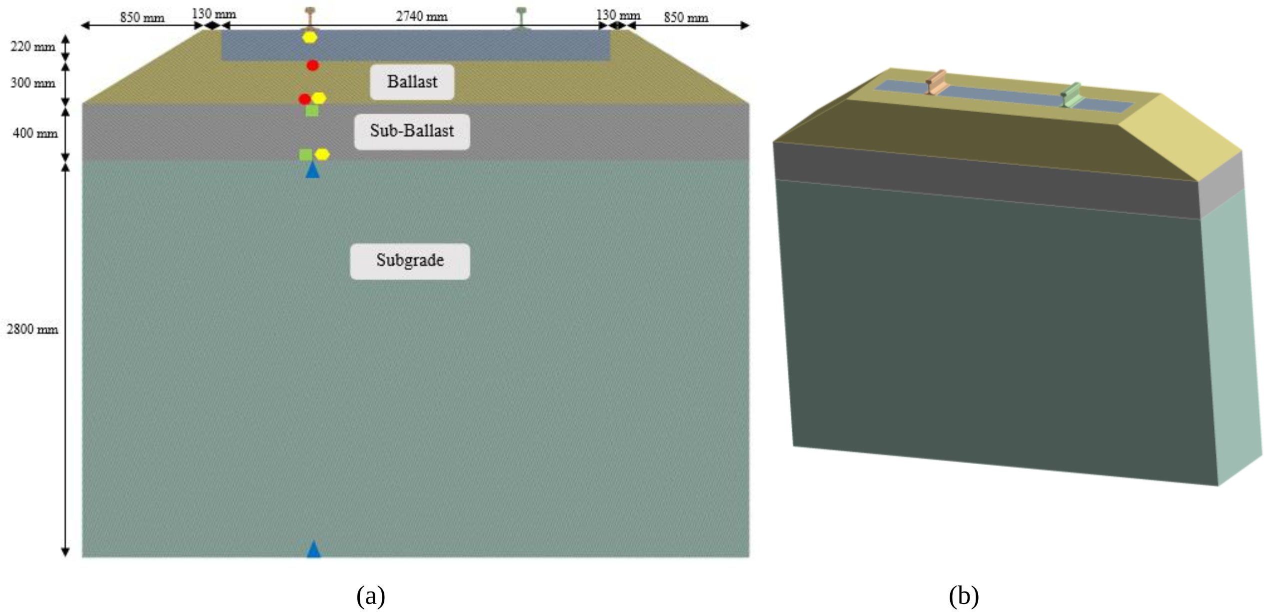

(a) (b)

- Strain-Stress at the top and bottom of ballast
- Strain-Stress at the top and bottom of sub-ballast
- Strain-Stress at the top and bottom of subgrade
- Deformation at the top of sleeper, at the bottom of ballast, and at the bottom of sub-ballast

Fig. 4 - Dimension Model of 1435 mm Gauge Railway Track: (a) Cross Section Model Dimension and Measuring Point; (b) 3D Model for Analysis

2.2 Railway Track Material Properties

Table 5 shows the material input used for the simulation. All materials in this study act to have linear elastic behavior. The parameter will be used for materials in this study are density, Young's modulus, and Poisson's ratio. The rail used for this study is R54 which is referred to UIC 54, while the sleeper uses concrete material. The material of rail refers to (Shahraki et al., 2015) while other materials refer to (M. Setiawan, 2022).

Table 5 - Material Properties for Simulation

Layer	Density (kg/m^3)	Young's Modulus (MPa)	Poisson's Ratio
Rail	6186	210,000	0.3
Sleeper	2300	29,100	0.3
Ballast	1900	130	0.2
Sub-Ballast	1900	120	0.3
Subgrade	2000	80	0.3

2.3 Railway Track Loading

The car used to be applied the load in this simulation is based on the double-stack cars manufactured by The GreenBrier Companies America, called 53' Husky-Stack as shown in Fig 5 (The GreenBrier Companies, 2019). This car can carry up to 53' containers in the bottom and top positions. Table 6 shows the weight specification of the car.

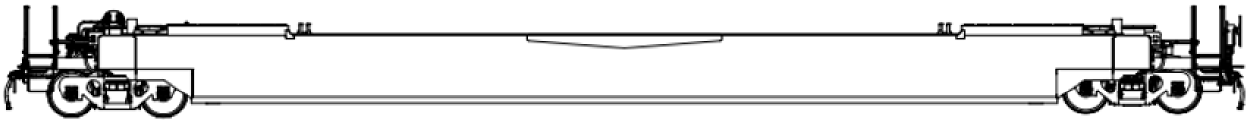

Fig. 5 - Car Type Used for Simulation

Table 6 - 53' Husky-Stack Weight Specification

Weight Type	Weight (lbs)	Weight (kg)
Light Weight	51,000	23,133
Capacity / Load limit	169,000	76,657

Gross Rail Road Capacity	220,000	99,790

As shown in Table 6, the maximum weight of a car is 99,790 kg, Fig. 5 showed that the car has 4 axles thus the load for every axle is 24,947.5 kg, which means that the wheel load is 12,473.75 kg. However, the load mentioned before is a static load where the load is present when the car is not moving. Then, calculate the dynamic load using Eq. 1 and Eq. 2 according to the Talbot formula (Rosyidi, 2015).

$$I_p = 1 + 0.01\left(\frac{V}{1.609} - 5\right) \quad (1)$$

$$P_d = P_s \; x \; I_p \quad (2)$$

Where *Ip* is the conversion factor, *V* is vehicle speed in km/h, *Pd* is dynamic wheel load, and *Ps* is static wheel load. To calculate the dynamic load, the speed factor and static load factor are essential. For example, with the speed of 60 km/h, within the equation above can be found that the dynamic load is 16,501.6 kg.

Table 7 shows the case scenario for the simulation based on the gauge length, speed, and other parameters explained above. The gauge length used for the analysis is 1067 mm and 1435 mm, while the speed varies from 60 km/h – 160 km/h. However, based on Indonesia's railway track technical requirements, the maximum speed of 1067 mm gauge is limited to 120 km/h, thus the speed of 160 km/h is only performed by 1435 mm gauge.

Table 7 - Case Scenario

Case Number	Gauge Length (mm)	Speed (km/h)	Car Axle Load (kg)	Wheel Static Load (kg)	Wheel Dynamic Load (kg)	Dynamic Load (N)
A1 A2	1435 1067	60	24,947.5	12,473.75	16,501.6	161,825
B1 B2	1435 1067	90	24,947.5	12,473.75	18,827.3	184,632.8
C1 C2	1435 1067	120	24,947.5	12,473.75	21,153	207,440.6
D1	1435	160	24,947.5	12,473.75	24,254	237,850.9

3. Results and Discussions

The analysis results in some output as mentioned in the previous part, that are deformation, stress, and strain of the track.

3.1 Track Layer Deformation

The deformation of every layer of the track can be known after the analysis. Fig 6 shows the behavior of the track for every load applied in 1435 mm gauge track, while Fig 7 shows the behavior of the track in 1067 mm gauge for every load.

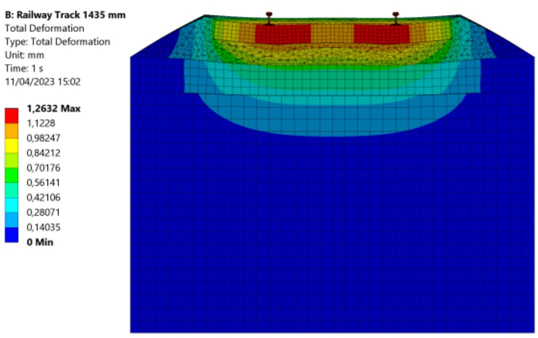

(a) Case A1

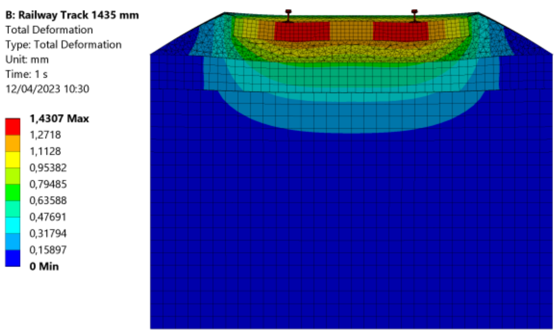

(b) Case B1

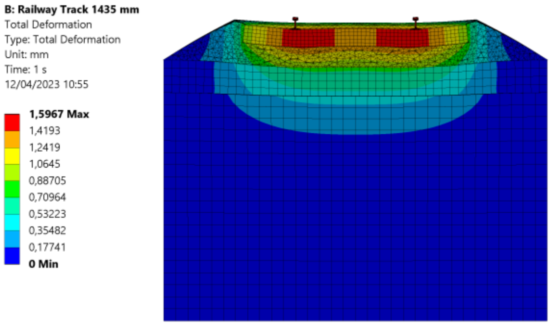

(c) Case C1

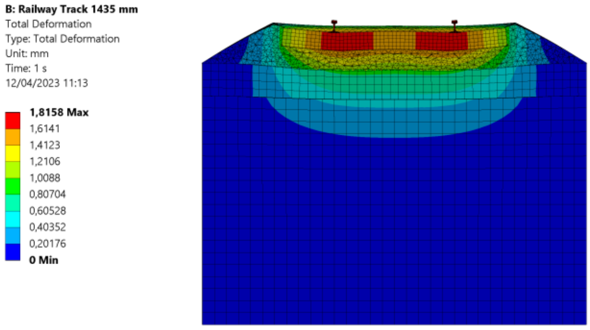

(d) Case D1

Fig. 6 - Deformation Distribution of 1435 mm Gauge Track

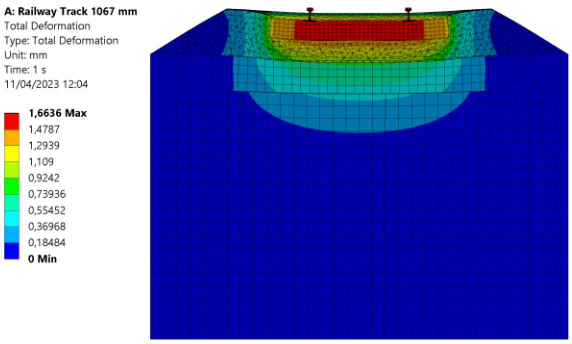

(a) Case A2

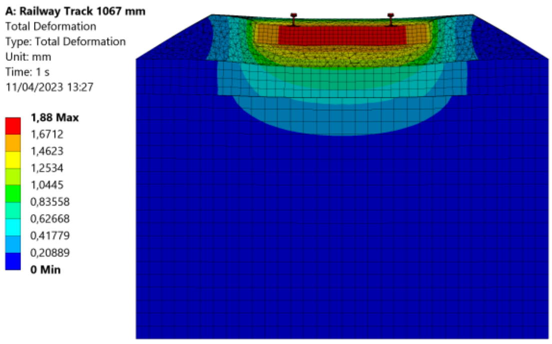

(b) Case B2

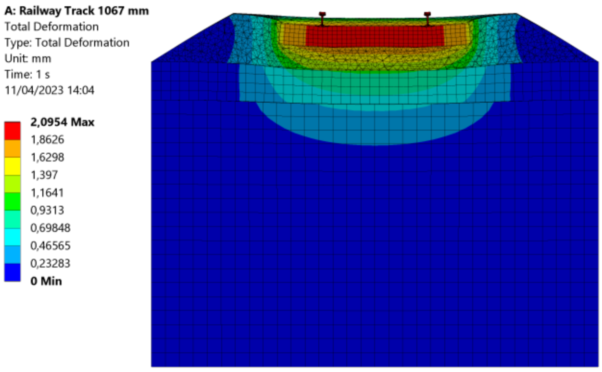

(c) Case C2

Fig. 7 – Deformation Distribution of 1067 mm Gauge Track

The pictures above represent the deformation distribution of the tracks. It can be seen that the deformation pattern of both 1435 mm gauge and 1067 mm gauge are similar. The roadbed layers look very similar, but if look closely at the pictures, the deformation on the sleeper is different. Deformation on 1067 mm gauge sleeper occurs on the whole sleeper, in contrast to 1435 mm gauge sleeper where the deformation occurs from the bottom of the rail and creeps to the middle of the sleeper. However, the deformation values for every case are different, especially for the 1435 mm gauge and 1067 mm gauge with the same load as shown in Fig. 8. It can be seen that the highest deformation happened in the top sleeper, followed by bottom ballast and bottom sub-ballast respectively. In addition, the deformation difference distance on 1435 mm gauge and 1067 mm gauge is around 0.4472 mm (32.8%) on average at the measurement point of the top sleeper, followed by 0.2181 mm (25.4%) and 0.0941 mm (22.3%) in bottom ballast and bottom sub-ballast respectively.

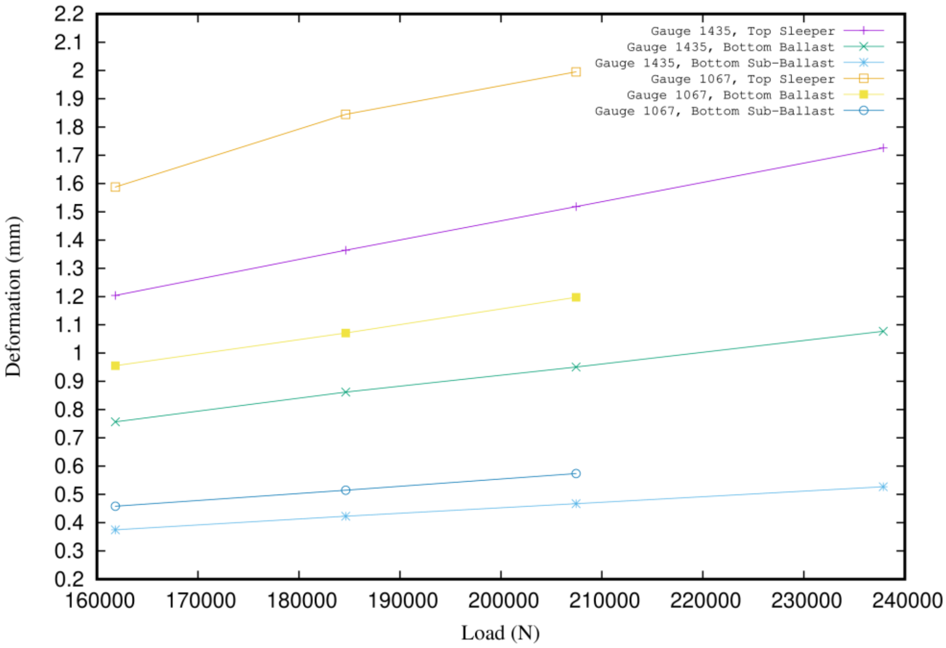

Fig. 8 - Deformation Measurement

3.2 Track Layer Stress-Strain

Stress-strain outputs are important to understand the mechanistic behavior of every layer of the railway track. It can illustrate the condition of the material under certain conditions. The stress distribution on the railway track is shown in Fig 9 for 1435 mm gauge and Fig 10 for 1067 mm gauge and the value of the stress is shown in the graphic in Fig 11, while the strain distribution is shown in Fig 12 for 1435 mm gauge and Fig 13 for 1067 mm gauge and the strain value shown on Fig 14.

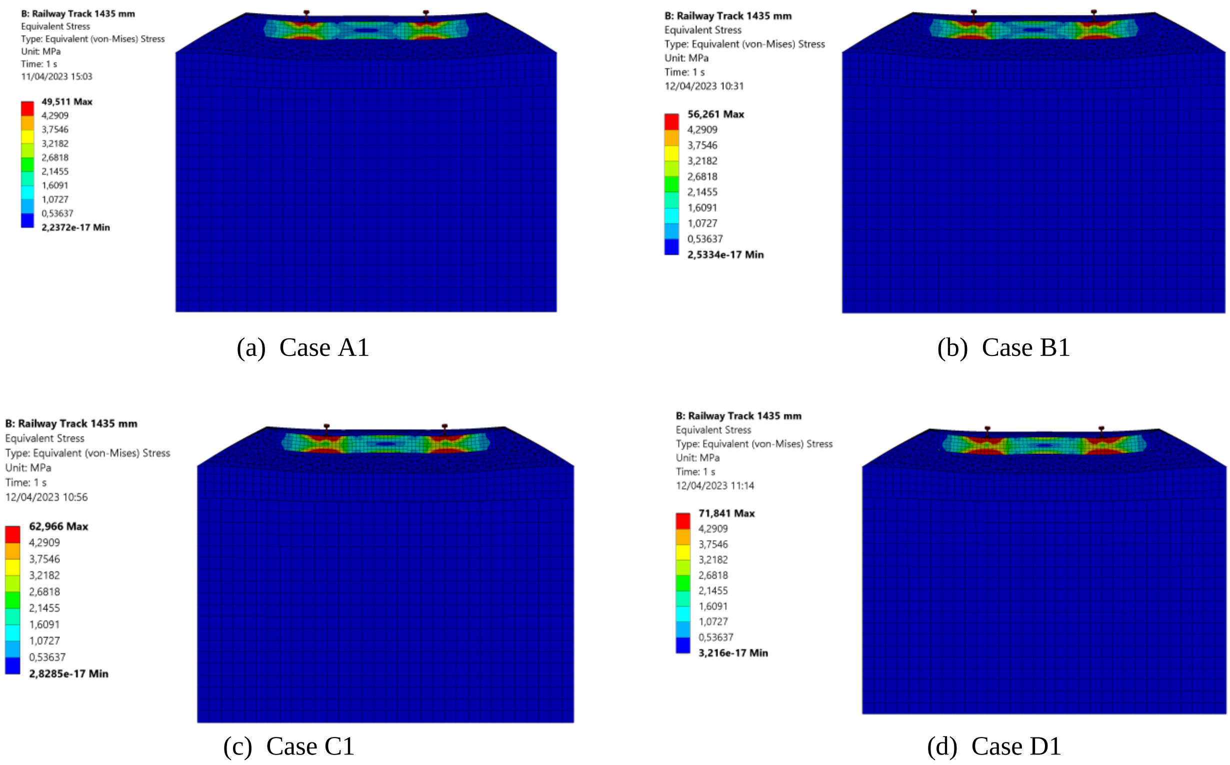

(a) Case A1 (b) Case B1

(c) Case C1 (d) Case D1

Fig. 9 - Stress Distribution of 1435 mm Gauge Track

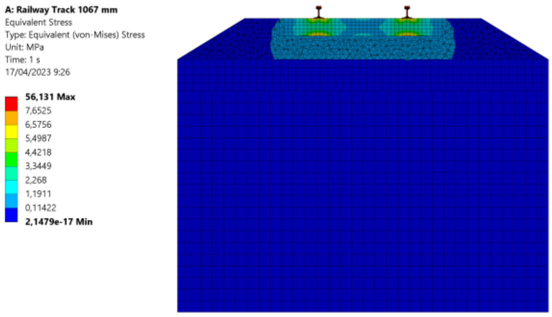

(a) Case A2

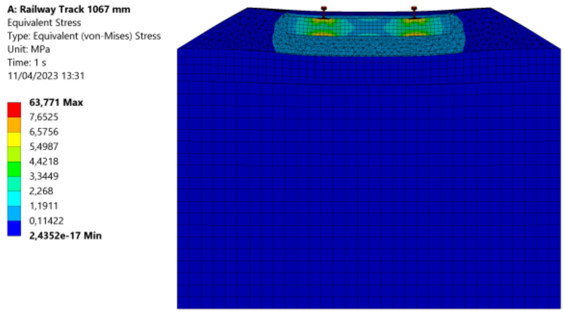

(b) Case B2

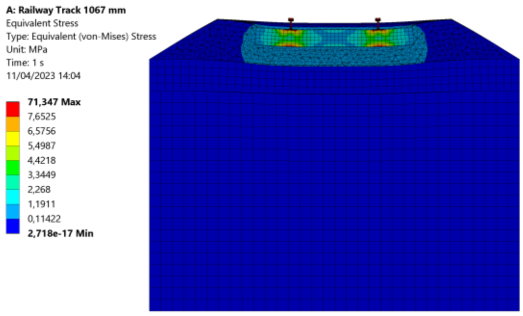

(c) Case C2

Fig. 10 - Stress Distribution of 1067 mm Gauge Track

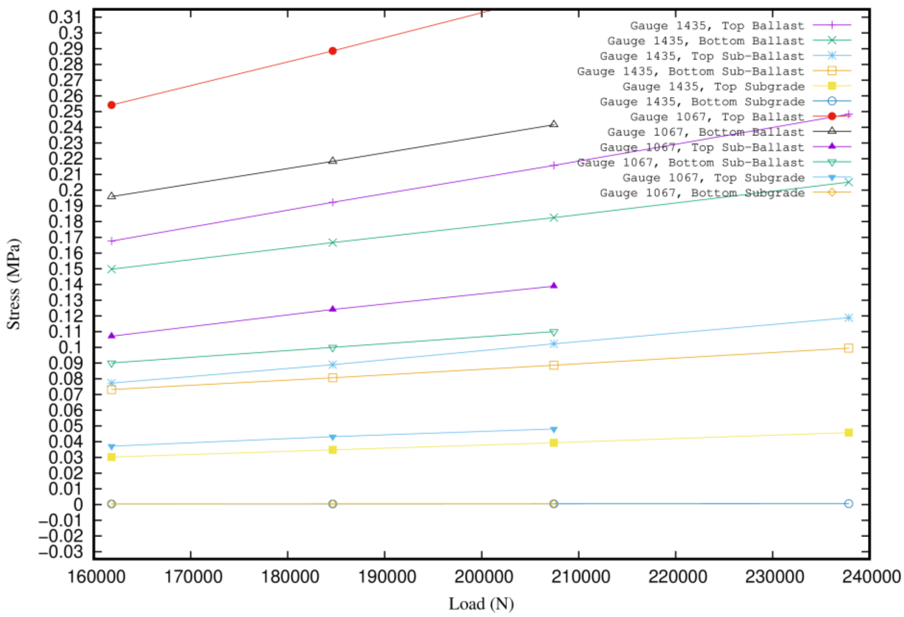

Fig. 11 - Measurement of Stress

Fig 9 and Fig 10 show that the stress is concentrated on the sleeper area because the sleeper impacted directly the load occurs in the rail. However, the sleeper is not included in the measurement of stress. The pictures above also show that stress on the ballast layer in 1067 mm gauge is more noticeable than stress in 1435 mm gauge. Fig 11 illustrates that stress in almost every layer is higher in 1067 mm gauge than 1435 mm gauge. The biggest stress happens in the Top Ballast of 1067 mm gauge with stress average is around 0.289 MPa, which is higher 0.083 MPa (40.4%) than 1435 mm gauge stress which is around 0.206 MPa in the same measurement position. This explains that a wider gauge can distribute the load evenly and cause the stress to occur in the layer underneath to become smaller. While the stress value on the bottom of the subgrade is almost the same, with a difference of about 0.000005 MPa.

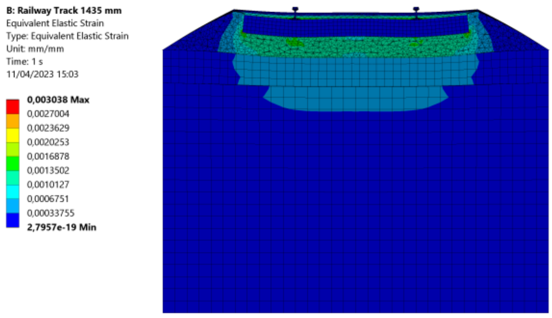

(a) Case A1

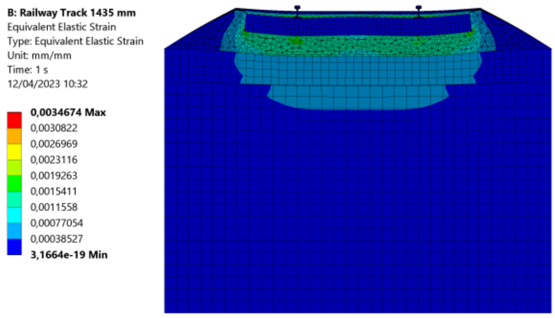

(b) Case B1

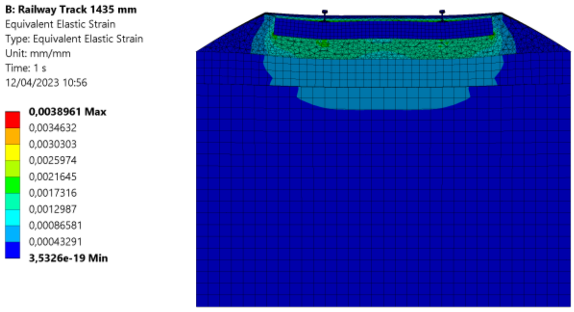

(c) Case C1

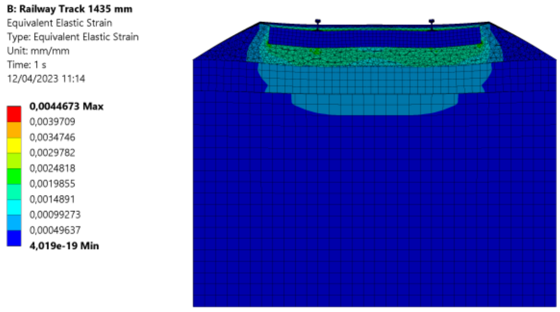

(d) Case D1

Fig. 12 - Strain Distribution of 1435 mm Gauge

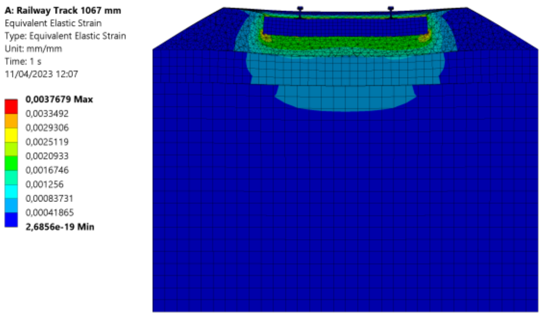

(a) Case A2

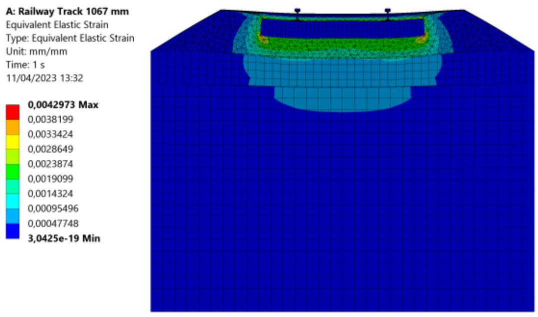

(b) Case B2

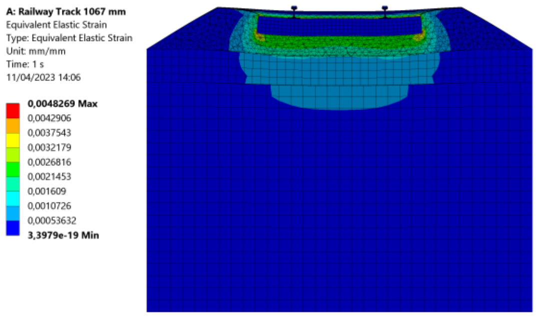

(c) Case C2

Fig. 13 - Strain Distribution of 1067 mm Gauge

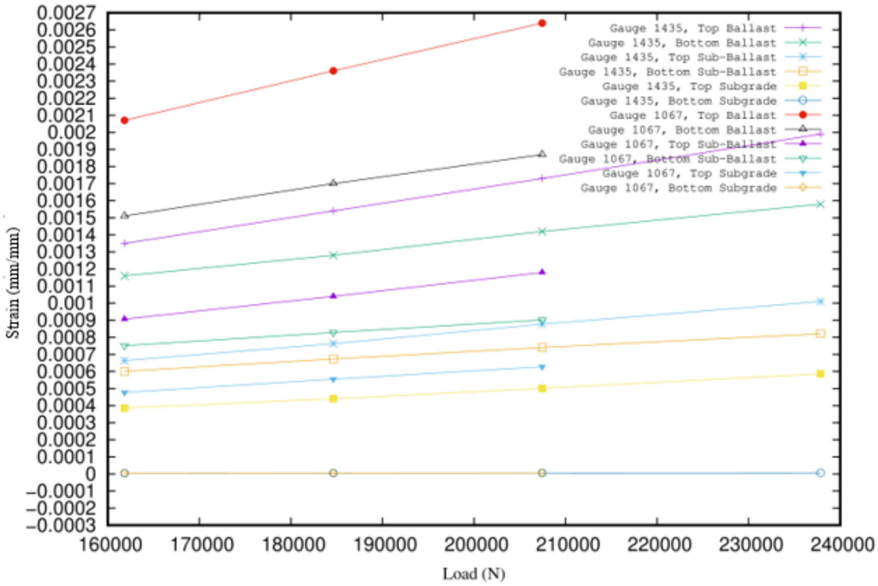

Fig. 14 - Measurement of Strain

The distribution of strain is almost the same between the 1435 mm gauge and 1067 mm gauge as shown in Fig 12 and Fig 13. However, the strain value are completely different. The strain value on 1067 mm gauge are higher than on 1435 mm gauge in every layer. On the top ballast position, the average strain value is 0.00236 mm/mm for 1067 mm gauge and 0.00165 mm/mm for 1435 mm gauge. It also can be concluded that the strain on 1067 mm gauge is 42.8% higher than the strain on 1435 mm gauge. It shows that the 1435 mm gauge can be more resilient than the 1067 mm gauge to withstand higher loads.

Stress and strain output is correlated to the modulus of elasticity or Young's Modulus (*E*). Table 8 explains the deviation between the measured elastic modulus calculated using Eq. 3 (Faridmehr et al., 2014) and the theoretical elastic modulus that has been entered in the properties material section. The measured elastic modulus is mostly slightly lower than the theoretical elastic modulus. This shows that there is little differentiation between the theoretical elastic modulus and measured elastic modulus in calculation using software simulation.

$$E = \frac{\sigma}{\delta} \tag{3}$$

Where E is the elastic modulus value (MPa), σ is the stress value (MPa) and δ is strain value (mm/mm).

Table 8 - Differences of Theoretical Elastic Modulus and Measured Elastic Modulus

Case	Layer	Theoretical Elastic Modulus (MPa)	Measurement Location	Measured Elastic Modulus (MPa)
A1	Ballast	130	Top	123.948
			Bottom	129.119
	Sub-Ballast	120	Top	116.429
			Bottom	121.692
	Subgrade	80	Top	78.432
			Bottom	83.012
A2	Ballast	130	Top	122.577
			Bottom	129.486
	Sub-Ballast	120	Top	118.080
			Bottom	119.967
	Subgrade	80	Top	77.791
			Bottom	75.301
B1	Ballast	130	Top	124.868
			Bottom	129.742
	Sub-Ballast	120	Top	116.720
			Bottom	119.896

	Subgrade	80	Top Bottom	79.164 78.883
B2	Ballast	130	Top Bottom	122.163 128.460
	Sub-Ballast	120	Top Bottom	119.001 120.843
	Subgrade	80	Top Bottom	77.848 73.621
C1	Ballast	130	Top Bottom	124.711 128.308
	Sub-Ballast	120	Top Bottom	116.614 119.704
	Subgrade	80	Top Bottom	78.353 81.697
C2	Ballast	130	Top Bottom	122.850 129.529
	Sub-Ballast	120	Top Bottom	117.399 121.960
	Subgrade	80	Top Bottom	76.678 76.892
D1	Ballast	130	Top Bottom	124.823 129.443
	Sub-Ballast	120	Top Bottom	117.336 121.214
	Subgrade	80	Top Bottom	77.932 80.340

3.3 Subgrade Service Life

Subgrade is one important layer located at the bottom of the railway track structure. It means that subgrade layer is the last layer to receive the load from the other layers above. Thus, it needs to know the resilience and service life of this layer regarding to the maintenance schedule due to the layer location is make it difficult to monitor the condition and maintain the structure, different from the other layers that are easy enough to monitor the condition and doing the maintenance because their's location is on the top part of the structure.

Before calculating the subgrade service life, it needs to know the allowable number of repetitions from the train load passing using Eq. 4, then the service life can be known using Eq. 5 (Rose et al., 2014).

$$N_d = 4.837\ x\ 10^{-5} \sigma_c^{-3.734} E_s^{3.583} \quad (4)$$

$$L = \frac{1}{\sum_{i=1}^{n} \frac{N_p}{N_d}} \quad (5)$$

Where,
N_d is allowable number of subgrade load repetition,
σ_c is compressive stress at the top of subgrade (psi),
E_s is elastic modulus of subgrade (psi),
L is service life of subgrade (years),
N_p is predicted number of subgrade load repetition in one year

To accommodate the service life needs to know the load repetition in one year. A car consists of 4 axles and it will be counted as 1 repetition in this calculation. If it is predicted that in one day will be 20 trainsets passing consisting of 30 cars, thus the calculation of repetition in one year is shown in Table 9 below.

Table 9 - Number of Repetition Calculation

Parameter	Value
Number of trainsets per day	20 trainsets/day
Number of cars per trainset	30 cars/trainset
Number of repetition per day	600 repetitions/day
Number of repetition per year (365 days)	219,000 repetitions/year

Table 10 shows the calculation of subgrade service life. Case with lower speed gives longer service life explain that speed giving a big influence on the dynamic load as shown in Eq 1. For example, case A1 with a speed of 60 km/h gives 61% longer service life than case B1 with 90 km/h speed on the same gauge width. However, at the same speed, 1435 mm gauge track gives a longer service load than 1067 mm. In case A1, 1435 mm gauge has 63.7% longer service life than 1067 mm gauge in case A2. It also can be seen that 1435 mm gauge can distribute the train load better thus the load received by the subgrade smaller and the compressive stress that occurs in the subgrade also become smaller. To conclude, the railway operator should consider the maximum speed of the train to minimize the damage to the subgrade before its time because it strongly influences the compressive stress impacted on the subgrade. Another way to improve the service life is by increasing the thickness of the ballast and sub-ballast layer (Prabawa & Primadiyanti, 2022) because the thickness layer of ballast and sub-ballast influence the load distribution and thus can decrease the compressive stress on top of the subgrade. Besides that, the ballast and sub-ballast thickness used in this analysis are the minimum requirement of Indonesia's regulation.

Table 10 - Calculation of Subgrade Service Life

Case	Compressive Stress on Top of Subgrade (MPa)	Compressive Stress on Top of Subgrade (psi)	N_d	Service Life (years)
A1	0.054008	7.8332	8127654.465	37.11
A2	0.061629	8.9385	4964849.832	22.67
B1	0.061358	8.8992	5047225.588	23.05
B2	0.069601	10.0948	3152372.705	14.39
C1	0.068236	9.8968	3394353.924	15.50
C2	0.077567	11.2502	2103341.834	9.60
D1	0.076745	11.1309	2188702.434	9.99

4. Conclusions

Operating the double-stack train is one way to increase the amount of freight transported with the train without increasing the number of trains operated. In consequence, it will add the load of the train that impacted the railway track structure. The ANSYS software is used to make 3D model and evaluate Indonesia's railway track structure under a load of the double-stack train with 1067 mm and 1435 mm gauge and several scenarios of speed as well. Several important findings can be summarized as follows:

1. Gauge of 1435 mm gives better performance in all parameters of deformation, stress, and strain than 1067 mm gauge in all scenarios. The difference deformation between 1435 mm gauge and 1067 mm gauge on average is 32.8% in the top sleeper, 25.4% in the bottom ballast, and 22.3 % in the bottom sub-ballast. In the position of the top ballast, the average stress on 1067 mm gauge is 40.4% higher than the stress on 1435 mm gauge. While the strain parameter shows that the top ballast on 1067 mm gauge is 42.8% higher than the strain in 1435 mm gauge.
2. The speed of the double-stack train affected the output of three parameters. Higher speed makes the dynamic load higher and it will increase the load that occurs on the railway track. Thus, in the implementation of the operation of a double-stack train, the operator should consider the maximum speed.
3. The 1435 mm gauge gives longer service life in all scenarios, with 37.11 years for the longer service life with speed of 60 km/h. While the 1435 mm gauge in speed of 160 km/h service life is 9.99 years, still longer than the 1067 mm gauge with 120 km/h speed which is 9.6 years. However, the operator should determine suitable gauge width and maximum operating speed to maximize the service life.

However, this paper only considers the static load, future research is needed to see the long-term structural behavior of the railway track under cyclic loading. The thickness component of ballast and sub-ballast is also important to decide the subgrade service life. It also needs to be considered possibility of reinforcing the soil on the input parameter to improve the service life of subgrade. Lastly, it also need the validation of the lab-scale test before the operation of the double-stack train.

Acknowledgement

The authors would like to thank the Research Center for Transportation Technology, Research and Innovation Agency of Indonesia which made this research possible.

References

Alam, F., & Watkins, S. (2007). Effects of crosswinds on double stacked container wagons. *Proceedings of the 16th Australasian Fluid Mechanics Conference, 16AFMC, March 2014*, 758–761.

Badan Pusat Statistik. (2023). *Jumlah Penumpang dan Barang Berdasarkan Moda Transportasi Kereta Api*. https://www.bps.go.id/indicator/17/2051/1/jumlah-penumpang-berdasarkan-moda-transportasi-kereta-api.html

Esveld, C. (2001). Modern Railway Tracks. In *MRT Productions* (Vol. 1, Issue 1). https://www.researchgate.net/publication/269107473_What_is_governance/link/548173090cf22525dcb61443/download%0Ahttp://www.econ.upf.edu/~reynal/Civil wars_12December2010.pdf%0Ahttps://think-asia.org/handle/11540/8282%0Ahttps://www.jstor.org/stable/41857625

Faridmehr, I., Hanim Osman, M., Bin Adnan, A., Farokhi Nejad, A., Hodjati, R., & Amin Azimi, M. (2014). Correlation between Engineering Stress-Strain and True Stress-Strain Curve. *American Journal of Civil Engineering and Architecture*, *2*(1), 53–59. https://doi.org/10.12691/ajcea-2-1-6

Kalliainen, A., Kolisoja, P., & Nurmikolu, A. (2016). 3D Finite Element Model as a Tool for Analyzing the Structural Behavior of a Railway Track. *Procedia Engineering*, *143*(Ictg), 820–827. https://doi.org/10.1016/j.proeng.2016.06.133

Kementerian Perhubungan. (2012). Persyaratan Teknis Jalur Kereta Api. *PM. No. 60 Tahun 2012*, 1–57.

Kementerian Perhubungan. (2018). Peraturan Menteri Perhubungan Republik Indonesia Nomor KP 2128 Tahun 2018. *Peraturan Menteri Perhubungan Republik Indonesia Nomor KP 2128 Tahun 2018*, 1–8.

Liu, S. (2013). *Kentrack 4 . 0 : a Railway Trackbed Structural Design*.

M. Setiawan, D. (2022). Evaluation of Indonesia's Conventional Track Performance Based on Mechanistic Approach. *International Journal of Sustainable Construction Engineering and Technology*, *16*(5), 185–201. https://doi.org/10.30880/ijscet.2022.13.01.017

Mantovani, S., Morganti, G., Umang, N., Crainic, T. G., Frejinger, E., & Larsen, E. (2018). The load planning problem for double-stack intermodal trains. *European Journal of Operational Research*, *267*(1), 107–119. https://doi.org/10.1016/j.ejor.2017.11.016

Michas, G. (2012). Slab Track Systems for High-Speed Railways. *MSc Thesis*, 95.

Muthohar, I., Sumi, T., & Sutomo, H. (2009). The Implementation and Impacts of PSO, IMO, and TAC Schemes on National Railways Reform in Indonesia. *Proceedings of the Eastern Asia Society for Transportation Studies Vol. 7 (The 8th International Conference of Eastern Asia Society for Transportation Studies, 2009)*, *7*, 54.

Ng, M. W., & Talley, W. K. (2020). Rail intermodal management at marine container terminals: Loading double stack trains. *Transportation Research Part C: Emerging Technologies*, *112*(December 2019), 252–259. https://doi.org/10.1016/j.trc.2020.01.025

Prabawa, H. I., & Primadiyanti, S. P. (2022). The Effect of Ballast And Sub-Ballast Thickness Variation on Subgrade. *10th International Conference on Sustainable Energy Engineering and Application (ICSEEA 2022)*.

PT. Kereta Api Indonesia. (2022). *Annual Report 2021 PT Kereta Api Indonesia*.

Rose, J. G., Liu, S., & Souleyrette, R. R. (2014). Kentrack 4.0: A railway trackbed structural design program. *2014 Joint Rail Conference, JRC 2014*. https://doi.org/10.1115/JRC2014-3752

Rose, J. G., & Souleyrette, R. R. (2016). *Kentrack 4.0: A Railway Trackbed Structural Design Program*. 1–14.

Rosyidi, S. A. P. (2015). *Rekayasa Jalan Kereta Api: Tinjauan Struktur Jalan Rel*. Lembaga Penelitian, Publikasi dan Pengabdian Masyarakat Universitas Muhammadiyah Yogyakarta (LP3M-UMY).

Ruf, M., Cordeau, J. F., & Frejinger, E. (2022). The load planning and sequencing problem for double-stack trains. *Journal of Rail Transport Planning and Management*, *23*(July), 100337. https://doi.org/10.1016/j.jrtpm.2022.100337

Setiawan, D. M. (2021). Structural response and sensitivity analysis of granular and asphaltic overlayment track considering linear viscoelastic behavior of asphalt. *Journal of the Mechanical Behavior of Materials*, *30*(1), 66–86. https://doi.org/10.1515/jmbm-2021-0008

Setiawan, D. M. (2022). Sub-grade Service Life and Construction Cost of Ballasted, Asphaltic Underlayment and Combination Rail Track Design. *Jordan Journal of Civil Engineering*, *16*(1), 173–192.

Shahraki, M., Warnakulasooriya, C., & Witt, K. J. (2015). Numerical study of transition zone between ballasted and ballastless railway track. *Transportation Geotechnics*, *3*, 58–67. https://doi.org/10.1016/j.trgeo.2015.05.001

The GreenBrier Companies. (2019). *53' Husky-Stack Specification*. https://doi.org/https://www.gbrx.com/wp-content/uploads/2021/06/53-Husky-Stack.pdf

The GreenBrier Companies. (2022). *Stacking Arrangement*. https://www.gbrx.com/railcars/maxi-stack-i-car/

Urban, J. (1987). Double-Stack Service: A Breakthrough In Transportation Technology. *Outlook '88 64th Agricultural Outlook Conference*, *1*(3), 1–22.